

Pressure Wave Propagation In The Aorta With and Without Sudden Occlusion

Philippe Tresson, Elise Nicolas, Philippe Vezin

Abstract The blood hammer effect is one of the supposed mechanisms for blunt traumatic aortic ruptures. In this study, the pressure in a pulsatile flow were recorded at different locations along the aorta. Two aortas were subjected to this pulsatile flow at a rate of 60 b.p.m, and a sudden occlusion at the distal part were applied. The pressure wave characteristics, amplitude and phase, were extracted with a Fourier series decomposition and compared with respect to the distance from the isthmus for the different harmonics. The experiments show that the maximum of pressure increased significantly (~11-14%) with the distance from the isthmus with occlusion. The occlusion has created a retrograde pressure wave at higher velocity (19 and 27 m/s) compared to the normal pressure pulse wave (4-5 m/s). This backwards pressure wave created a short-lived overpressure (2 cardiac pulses) that also decreased to the isthmus. The maximum pressure of this wave (~18 kPa maximum) was lower than the level reported in literature (~100 kPa) and was not sufficient to create a rupture under the tested conditions. The geometry of the aorta (diameter, taper shape, curvature of the arch, etc.) had an influence on the characteristics of the pressure wave. However, the present study reproduced, with some limitations, a water hammer and analyse its propagation along the aorta under physiological conditions.

Keywords Aortic isthmus, blunt traumatic aortic rupture, occlusion, pressure wave analysis, reflective wave,.

I. INTRODUCTION

Blunt traumatic aortic ruptures (BTAR) are traumatic lesions of the thoracic aorta as a result of blunt trauma and represent the second cause of death related to road accidents after head trauma [1]. BTAR mainly occurs at the aortic isthmus that may be the weaker part of the aorta [2-4]. The isthmus represents the junction between the mobile part of the aorta (the ascending aorta and the aortic arch) and the fixed descending aorta (the thoracic aorta). Several hypotheses for the pathogenic aetiology were issued regarding anatomic and mechanical factors but the kinetic energy in high-speed deceleration mechanism or thoracic blunt traumatic injury seems an essential factor, but not alone, in the development of BTAR. Reference [5] suggest that posteriorly directed acceleration alone (up to 80g during 20s) is not sufficient to cause aortic injury. Whereas, in their experiments, their recorded overpressure higher than 100 kPa that was found to correspond to 50% of aortic injury risk [6]. This latest author concluded that this peak pressure at failure showed that the pressure mechanism could be sufficient to produce aortic failures under realistic pressure loading. They also conclude that, due to the pattern of the observed ruptures that sometimes differ from the epidemiological literature; the pressure mechanism may not be the only cause of aortic rupture.

A unique mechanism is often described such as deceleration, aortic stretching, intravascular pressure, osseous pinch, or the blood-hammer effect. However, BTAR was described as a more complex mechanism involving several processes [1]. Deceleration alone was found not sufficient and probably thoracic deformation is required [5]. In human cadaver tests under dynamic and quasi-static configurations, [7] reproduced the aortic injuries at peri-isthmus. They proposed the tethering of descending aorta by the pleura to be the primary contribution to BTAR rather than the aortic intraluminal pressure or the body acceleration. Same authors conducted additional tests under various blunt loadings, and concluded the aortic longitudinal stretch resulting from thoracic compression to be the primary cause of BAR [8].

P. Tresson is PhD student in Biomechanics at University of Lyon, University Gustave Eiffel, University Claude Bernard Lyon 1, LBMC UMR_T 9406, F-69622 Lyon, and cardiovascular surgeon at Hospices Civils de Lyon, Hôpital Louis Pradel, Service de chirurgie vasculaire et endovasculaire, Hôpital Louis Pradel, F-69677 Bron Cedex, France (Phone: +33 04 72 11 09 90, philippe.tresson@chu-lyon); E. Nicola is a Master degree student, P. Vezin is senior researcher in Biomechanics at University of Lyon, University Gustave Eiffel, University Claude Bernard Lyon 1, LBMC UMR_T 9406, F-69622 Lyon, France.

The most observed rupture is a transverse tear of the aorta[9][10]. Irrespective of the mechanisms, BTAR is a rupture of the aortic wall with an arterial tear extending from the intima to the outermost layers; the force acting from the inside towards the outside [11][12]. BATR often leads to death; for example, in road accidents 85% of victims die at the scene of the collision [13]. Without treatment, 30% of the remaining injured will die within 24 hours. If BTAR is diagnosed, an endovascular exclusion with a thoracic endovascular repair can be performed to prevent a secondary haemorrhagic rupture.

Among the different mechanisms studied, BTAR was proposed, as the result of a blood-hammer effect [2]. The effects of an overpressure for the rupture of the aorta have been discussed for many years; [2] first give a good review. This hypothesis suggests that blunt trauma causes occlusion of the diaphragmatic orifice where the aorta passes from the thoracic to the abdominal cavity, resulting in a reflected intraluminal pressure wave of a non-compressible fluid leading to maximum effect at the aortic arch. This would be expected to be significantly greater at the aortic arch because of the curvature reflecting and intensifying the pressure wave. This pressure wave could be associated with a strain wave occurring in the hyperelastic wall of the aorta where part of the wall is suddenly stretched faster than it can be elongated which leads to aortic rupture [2][14].

If the aorta was an isotropic cylindrical vessel, it would theoretically rupture axially rather than transversely under intravascular pressure. According to [1], a transverse rupture could occur if the ratio of the transverse to longitudinal strength is at least 2:1. Bi-axial [15] or inflation tests [13] show results that confirm this theory.

Reference [16] has demonstrated that, during acceleration, a blood mass transfer occurs from the distal half of the thoracic aorta to the upper half of the arch. This retrograde flow may increase the pressure sufficiently in the region of the arch to cause rupture. This phenomenon of blood mass transfer is different from a pure pressure wave propagation. The effect of such an acceleration or of a pressure wave propagation due to a sudden occlusion of the blood flow has been studied using analytical models [17-19]. However, these analytical studies did not consider the additional deformation of the aorta during an impact where the increase in the curvature of the arch could possibly lead to greater increases in the pressure wave in this anatomic region. Even without considering this increased curvature effect, the analysis of axial wall strain and strain rate indicates that wave propagation resulting in high-pressure wave propagation along the aortic wall can lead to transverse ruptures since the relatively high rate displacement mechanism increases the stress in the axial direction [12][6].

An intra-aortic retrograde high-pressure wave due to blunt impact or sudden occlusion is similar in waveforms and propagation speed to the retrograde pressure wave highlighted in cardiovascular physiology. Anterograde and reflective pressure waves have been described in the cardiovascular system as the contraction of the left ventricle, which induces a sudden pressure wave in the blood mass and propagates in the large vessels in the form of a parietal wave. It appears before the pulsatile blood flow with a velocity of 5.0 m/s while the blood mass flows more slowly (0.4-1 m/s) [20]. A rise in resistance occurs when passing from the large arteries to the arterioles or through bifurcations of the arterial tree, i.e., separation of the descending aorta into left and right iliac arteries, and leads to a reflection of the parietal pressure wave. When the reflective pressure wave returns towards the heart, it crosses and superimposes on the blood flow wave. The velocity of systemic arterial waves can allow reflection activity to return to the aorta during the same systolic period, increasing peak systolic pressure and worsening the left ventricular afterload conditions. These arterial pulse wave reflections may be essential in determining the shape of the pressure and flow waveforms in the aorta [20-22].

Peripheral vascular tone is the main factor determining the magnitude of reflected pressure waves from the peripheral circulation to the ascending aorta [23-25]. Different reflecting sites may produce a summated reflected wave that appears to arise from a single reflecting site. However, regional peripheral vascular tone within the abdomen and trunk is considered as the main origin of pressure wave reflection activity throughout the systemic arterial system [23][24]. By analogy, a retrograde pressure wave could be triggered during blunt trauma after an impact or after an acute occlusion of the diaphragmatic orifice. These latter could lead to the reflective pressure wave by a brutal stop of blood flow. In addition, occlusion of the thoracic aorta due to osseous pinch and mediastinal displacement (shovelling effect) combined with other physiological factors such as hypertension, cardiopulmonary dynamics at the time of impact, a catecholamine surge, or the association with the anterograde wave may contribute to worsen the pressure wave.

To our knowledge, there is no recent experimental study using cadaverous (human or animal) model or bench tests that have enabled to reproduce this mechanism with realistic blood flow conditions, e.g., time-varying flow, or found a reflection wave after a blunt trauma. We hypothesise that after the occlusion of the aorta, local

pressure reflective waves, traction, and strain waves in the arterial wall act simultaneously and explain why ruptures are nearly always transverse and preferentially located in the isthmus region. To demonstrate this hypothesis, the present experimental study aimed first to measure and describe the “normal” (i.e. physiological) pressure wave along the aorta without an abdominal occlusion. Then to assess whether a sudden occlusion of the thoraco-abdominal aorta creates a retrograde wave pressure and modify the normal pressure wave. For that purpose, the pressure of a simulated haemodynamic flow was measured at different locations along the aorta to detect and to analyse the reflective pressure wave and its progression along the aorta.

II. METHODS

Specimen Preparation

The cardiopulmonary system of pigs, including the heart, the lungs, the trachea, the pulmonary arteries, the inferior vena cava (IVC), the superior vena cava (SVC), the thoracic aorta with the ascending aorta, the aortic arch with the first centimetres of the supra-aortic trunks and the descending aorta was instrumented to reproduce the cardiopulmonary circulation. These biological materials came from a local butcher. The age and weight of the pigs were not provided. But being common pigs for consumption, the average age and weight is around 6 months and 115-120 kg. The cardiovascular systems were immediately stored in a freezer (-18°C) until their use. Samples were thawed at room temperature (19°C) before their preparation.

For the catheterisation of the cardio-pulmonary circulation, the model was prepared as follows. The connective tissues around the aorta and the carotids were removed. The ligamentum arteriosum, that connect the aorta with the pulmonary artery and the connective tissue around it and in the zone of contact between these two vessels were kept. The extremity of the SVC, the azygos vein and the left common carotid were ligated with two 5/0 thread monofilament sutures. After the dissection, the IVC and the ascending aorta were catheterised for the connection to the circulatory system. A cannula was inserted at the pointed tip of the left ventricle for the systemic circulation. A small aperture was performed on the left ventricle and the cannula with a profiled end cap was inserted through this passage. A suture with a monofilament, reinforced by a pericardium patch to avoid a muscle tearing, maintained a good patency and prevented the cannula from being extracted due to the flow. Another cannula was inserted in the IVC for the pressurisation of the pulmonary arteries. A simple ligature around the IVC facing the cannula ensured the sealing. The outflow cannula was inserted in the descending thoracic aorta and attached to a single wire. All handling procedures were carried out in accordance with the guidelines of the LBMC laboratory for biological material handling. Since the samples came from a butcher, ethical review was not required.

Test Set-up

A specific mock circulatory loop was designed to mimic and monitor aortic haemodynamical flow with reasonable accuracy by reproducing pulse rate, and pressure conditions (Fig. 1.). The aorta circulation consisted of successive elements, which looped the fluid between a tank and the aorta. The tank, open to the atmospheric pressure, contained the fluid (water at 19°C for the present study but blood mimicking fluid (BMF) can also be used) and was connected to a pumping system. The pump and a proportional solenoid valve (Posiflow 203, ASCO Numatics) allowed to reproduce the pulsatile flow. The successive valve opening and closing (corresponding to systole and diastole) controlled the pulse. An ultrasound flowmeter (SU7000, Ifm electronics) measured the inlet flow during the tests. The flowmeter was placed on a horizontal straight section of a pipe with a sufficient length to ensure the stabilisation of the flow.

Pressure sensors, having a miniature design of \varnothing 6.4 mm and length 11.4 mm (EPB-PW 3.5 Bar, TE Connectivity), were placed in the aortic arch and along the thoracic aorta either by the intercostal arteries or by a small hole into the aortic wall to measure the pressure continuously (Fig. 1. Right). A ligature ensured the sealing around the sensor. The size of sensors were small enough to avoid perturbations of the flow and to avoid interferences between them due to their wakes. It was checked by comparing the measurement of the sensor at the distal end of the aorta with and without the other upstream sensors

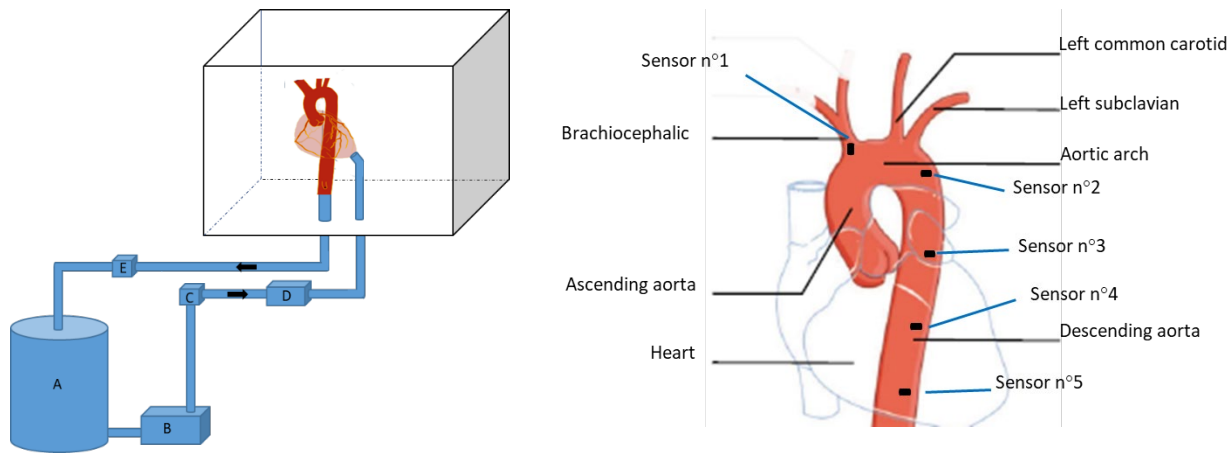


Fig. 1. Schematic representation of the mock circulatory loop. A: Tank, B: Pump, C: Solenoid valve, D: Flowmeter, E: Ball valve and Location of the pressure sensors along the thoracic aorta. It should be noted that pigs have only two carotids instead of three for humans. Illustration adapted from Servier Medical ART (smart.servier.com).

A custom-made LabVIEW SignalExpress (National Instrument) programme controlled the solenoid valve. Downstream of the aorta, ball valves were used to simulate peripheral vessels resistance. The closing degree of the valves allowed to set the physiological pressure level in the aorta. In this configuration, a compliant Windkessel chamber was not required. In the literature, it was common to add such a chamber to dampen the flow and to adjust pressure but most of these studies were conducted on rigid phantoms [26][27]. In the present case, the pig aorta compliance was sufficient to recreate the flow dampening effect (Fig. 2).

The cardiopulmonary system was fixed on a rigid support and placed in a rectangular glass container (at atmospheric pressure) to prevent from projection when the rupture of the aorta occurred and to collect any leaks during the tests. The support allowed keeping the position and orientation of the different parts of the cardiopulmonary system close to the physiological conditions. The cardiopulmonary system was held vertically. A wire was passed around each bronchial stump and fixed to a horizontal bar to hold the lungs. The trachea was fixed to the same horizontal bar. The heart rested on a flat surface. There was no other fixation for the supra aortic trunks which was ligated for sealing.

Each specimen was preconditioned first by applying a constant flow rate to fill all the vessels and check for any leaks. Then the pulmonary arteries were clamped. The aim was to reproduce as close as possible the boundary conditions and constraints of the aorta that is connected with the pulmonary artery by the ligamentum arteriosum. Then the aorta specimen was subjected to a pulsatile flow rate, Q , similar to an average adult flow rate [28] (Fig. 2.). The duration of the pulse was 1 second and was repeated several times. Then, a specific electro pneumatic device created a sudden occlusion at the distal extremity of the descending thoracic aorta (between sensor 4 and 5). The device consists of a horizontal small plate placed in the front of the descending aorta and mounted on two small pneumatic jack (one at each end of the plate) triggered by compressed air. This pushes quickly the plate back and pinches the aorta between the plate and the support at the back of the aorta. This occlusion aims to produce a high-pressure wave, i.e., a water-hammer effect, in the aorta that is superimposed and interacts with the reflective pressure wave.

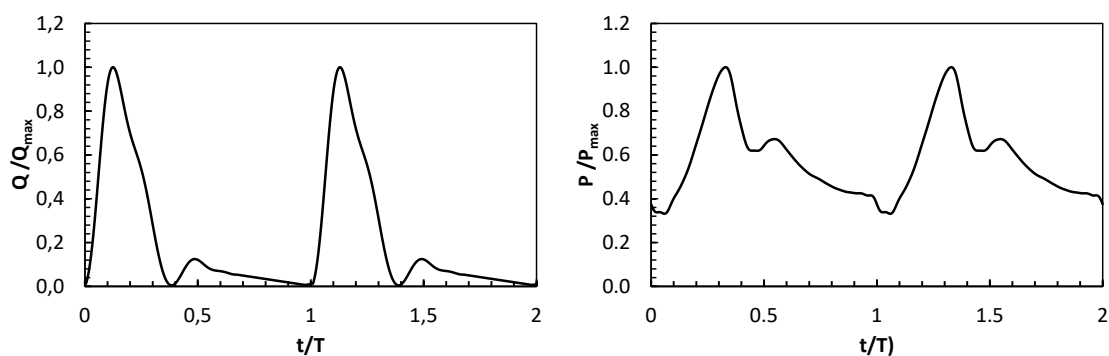


Fig. 2. Typical blood flow waveform (left) and pressure waveform without occlusion from sensor n°1 (right) obtain with the mock circulatory loop.

Data Processing and Analysis

Analog signals from the pressure sensors and flowmeter were recorded at a sample frequency, f_s , of 2,000 Hz with the LabVIEW SignalExpress programme over a duration of 120s. During each recording, the first 20 seconds are to ensure that the flow is correctly established and to check visually for any leaks or other malfunctions. Then the 40 following cycles (40 seconds) were used to extract information about the physiological pressure wave, while the last 60 seconds were used to analyse the occlusion of the descending aorta. The inlet conditions being periodic (successive valve opening and closing), it was observed that the flow and the pressure were also periodic. Theoretically, any periodic function, $S(t)$, can be expressed using a Fourier series (1) which frequencies are multiples, harmonics, of the main frequency (cardiac frequency in our case).

$$S(t) = a_0 + \sum_{i=1}^N a_n \cos(n\omega t) + \sum_{i=1}^N b_n \sin(n\omega t) \quad (1)$$

Where ω is the pulsation (rad/s), a_n is the coefficient of the Fourier series for the n^{th} harmonic. Equation (1) can be rewritten as:

$$S(t) = A_0 + \sum_{i=1}^N A_n \cos(n\omega t - \phi_n) \quad (2)$$

Where $A_n = \sqrt{a_n^2 + b_n^2}$ and $\phi_n = \text{atan}(b_n/a_n)$ are the amplitude and the phase of the n^{th} harmonic, respectively.

Previous researches [29][30] have shown that the first five harmonics (also called frequencies) contain over 90% of the energy of the pressure waveform. A series of 10 to 15 harmonics is assumed to contain more than 99% of the energy (in other words the Parseval's relation is verified with 10-15 harmonics) and is usually sufficient to adequately reconstruct waveforms in cardiovascular applications. A higher order Fourier series does not provide significant differences in the reconstructed pressure signals. Then any characteristic of the system response can be determined separately for each harmonic by the description of their amplitudes and their phases. The computation of the Fourier series, up to the 25 harmonic, was performed with an in-house Matlab programme. In the present study, only the four first harmonics are discussed since the 5th harmonic and higher represent less than 1% of the 1st harmonic. Prior to the Fourier analysis, the phase average (5) is computed to determine a mean signal of the 40 cycles.

$$\langle P_i \rangle = \frac{1}{M} \sum_{k=1}^M P(i + kT \cdot f_s) \quad (3)$$

Where i is the discretised time step ($i = 1, T/f_s$), M is the total number of pulses, f_s is the sampling frequency (Hz) and T is the signal period (s).

The sensors were placed equidistant as much as possible. As a result, it is reasonable to compare the amplitudes and the phase angles at each position along the aorta for the four harmonics. In the following, the distance of each sensor, d_i , is given relative to the first sensor. This sensor is inside the left carotid for all the tests and close to the aortic arch. It serves as position reference, ($d_1 = 0$). The amplitudes and phase angles were also normalised to the values of the 1st harmonic of the 1st sensor for each harmonic. We defined the amplitudes and phase for the the n^{th} harmonic of the i^{th} sensor ($i = 1, 5$) \tilde{A}_{in} and $\tilde{\phi}_{in}$ as:

$$\tilde{A}_{in} = A_{in}/A_{11} \text{ and } \tilde{\phi}_{in} = \phi_{in} - \phi_{11} \quad (4)$$

\tilde{A}_{in} and $\tilde{\phi}_{in}$ represent how the pressure pulse change along the aorta. Moreover, $\tilde{\phi}_{in}$ can provide an estimation of the velocity of the pressure wave appears to be traveling. This velocity is called the apparent phase velocity C_a and can be determined from the pulse frequency multiply by the ratio of the distance between to sensor with the phase lags.

III. RESULTS

The results from two aortas are presented in this section. The Fourier analysis for the pressure wave before the occlusion provides the baseline for the general pattern of the wave pressure propagation. Both tests showed similar harmonic patterns

The inner diameter and the wall thickness of the aorta at the location of each sensor were measured after each test (Table I). The geometrical data show the tapered shape of the aorta (decrease of the diameter from the proximal to the distal position). The second aorta had lower inner diameters D_i . The wall thickness, e_i , was relatively similar between the two aortas. Consequently, the shape ratio e_i/D_i was greater for the 2nd aorta. The local characteristics of the pressure wave, especially the reflective wave, depend on the local area of the aorta. Both the variation in time of the section of the aorta and the shape ratio have an influence. These differences could be important for the results of the amplitude, phase or apparent velocity of the pressure wave.

TABLE I
DIMENSIONS OF THE AORTA AT THE LOCATION OF THE PRESSURE SENSORS

Sensors	Sensor location		Diameter		Wall thickness		Shape ratio	
	d (mm)		D (mm)		e (mm)		e/D	
	Test 1	Test 2	Test 1	Test 2	Test 1	Test 2	Test 1	Test 2
1	0	0	21.3	19.7	2.9	3.1	0.136	0.157
2	60	55	17.4	14.1	2.6	2.6	0.149	0.184
3	110	110	17.2	13.9	2.4	2.3	0.140	0.165
4	150	160	16.1	13.5	2.2	2.2	0.137	0.163
5	200	222	15	12.8	2.1	2	0.140	0.156

Fig.3 shows the changes in amplitudes and phase angles of the first four harmonics of the pressure wave, without occlusion, between the proximal aorta (isthmus) and distal aorta of the two samples tested as a function of d_i . In all the tests the fourth sensor malfunctioned (despite being checked before and after the tests). It is clear that the amplitude and phase were a function of both frequency and location. For both tests, the amplitude of the pressure decreased with the frequency (harmonics) as expected. However, there were variations between the two aortas in pressure amplitudes along the aorta. The amplitude of the two first harmonics of the first test tended to increase toward the distal end. For the second test, the amplitude remained constant or decreased distally, except for the 2nd location where a slight increase of the amplitudes was observed for all harmonics. This behaviour was also observed for the 3rd harmonic in test n°1 and to a lesser degree for the 4th harmonic.

Fig. 3. shows that phase angles varied with the distance. Despite some fluctuations, the phase lag between the 1st harmonic and the three others tended to decrease between the sensors 1 and 2 and then increased slightly or reach a plateau distally for both aortas. The two tests also showed a similar trend when the frequency dependency was analysed. The phase lag with the 1st harmonic increased for the 2nd and the 4th harmonics but decreased with the 3rd one.

The occlusion, i.e., a sudden interruption of the flow, strongly modified the pattern of the pressure and an additional reflective pressure wave with a higher frequency is visible (Fig. 4.) on the curves of each sensor for both tests. The pressure increased during the cycle where the occlusion was applied and during the following cycle. The maximum pressure increased from 15.9 kPa (that correspond to the normal systolic pressure) to 17.8 kPa for the sensor 1, from 15.7 kPa to 17.7 kPa for sensor 2 and from 14.3 kPa to 16.3 kPa for sensor 3 (Fig. 4., left) for the 1st test. The variation were lower for the 2nd test: only from 12.1 kPa to 12.3 kPa for sensor 2 and from 11.0 kPa to 14.1 kPa for sensor 3 for the 2nd test (Fig. 4., right). The peak pressure, for the 1st sensor of the 2nd test, corresponding to the additional wave during the occlusion was only 11.4kPa while the maximum pressure was 11.9 kPa corresponded to the systolic pressure. All these peaks were reached during the 1st cycle following the occlusion.

The frequency of this additional wave decreased with the distance from the occlusion site. There were fewer differences between sensors 1 and 3 than sensors 2 and 3 due to the lower distance between the first pair of sensors. The frequency ($1/\Delta t$) also seemed to increase during the cycle where the occlusion was applied (Fig. 5). On the 1st cycle after the occlusion, the pressure wave was only visible through the maximum of pressure. After two flow pulses following the occlusion, this additional pressure wave had completely vanished. It is important

to explain that, in our experiment, the occlusion was not permanent, and under the action of the continuous flow of the pump, the section of the aorta was progressively opened again and allow the normal flow to resume after a maximum of two cardiac cycles.

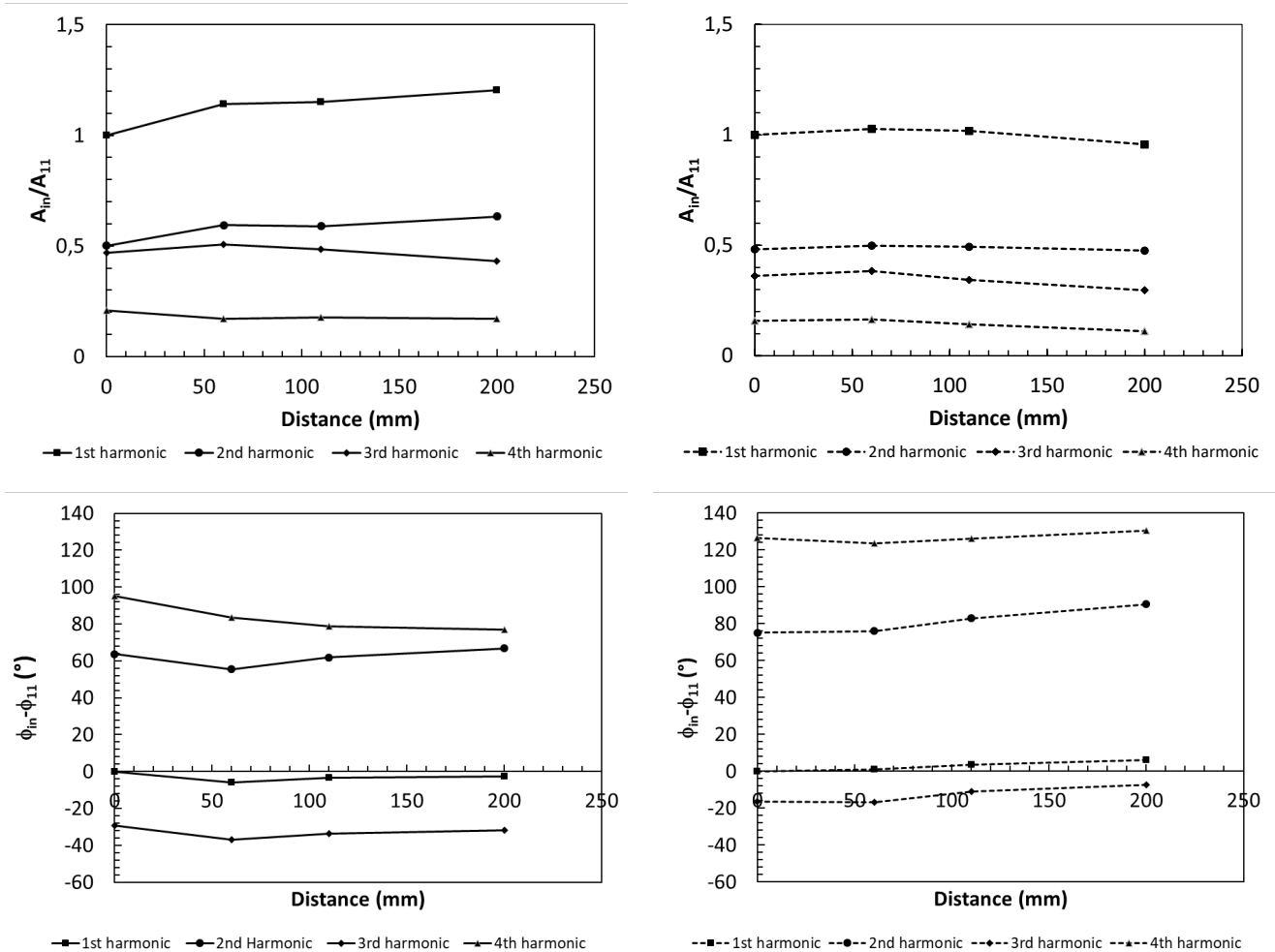


Fig. 3. Pressure amplitude (top), phase angles (bottom) along the aorta for the four first harmonics, test 1 (left) and test 2 (right).

Assuming the linearity of the system as a first approximation [34], one can consider that the retrograde pressure wave resulting from the occlusion is added to the normal pressure wave. Consequently, the Fourier analysis was also applied to the pressure wave during the cycle of the occlusion. Similarly, to the normal pulse wave, Fig. 6 shows the changes in amplitudes and phase angles of the pressure wave as a function of the distance. Comparing with Fig 3, the increase of the amplitude of the pressure was more important than without occlusion. This can be observed for all the harmonics even if for the 4th harmonic, the increase was only for the first two locations. It should be noted that the more distal location (sensor 5) was below the occlusion site. A similar pressure wave was observed at this location, but not presented here. This wave was a forward pressure wave with a similar pattern to the reflective wave. Such an increase was already noted during a bilateral femoral artery occlusion on patients [33]. There was no significant effect of the occlusion on the phase angles between the pressure waves with or without occlusion.

The pressure wave velocity and impedance depend on material properties, fluid density and the shape ratio of the vessels. However, the comparison of the time of the maximum pressure along the aorta (See Table II) can provide an approximation of the propagation time of the effect of the pressure wave after the occlusion on the pressure wave due to the flow. It appears clearly that the maximum of pressure occurred early close to the occlusion site and travelled backwards along the aorta. The results from Table II suggest that the retrograde pulse velocity averaged about 19 m/s in test 1 and 27 m/s in test 2. The differences between the two tests could be explained partly by the differences in the shape ration (see Table I) that have an influence on the wave velocity.

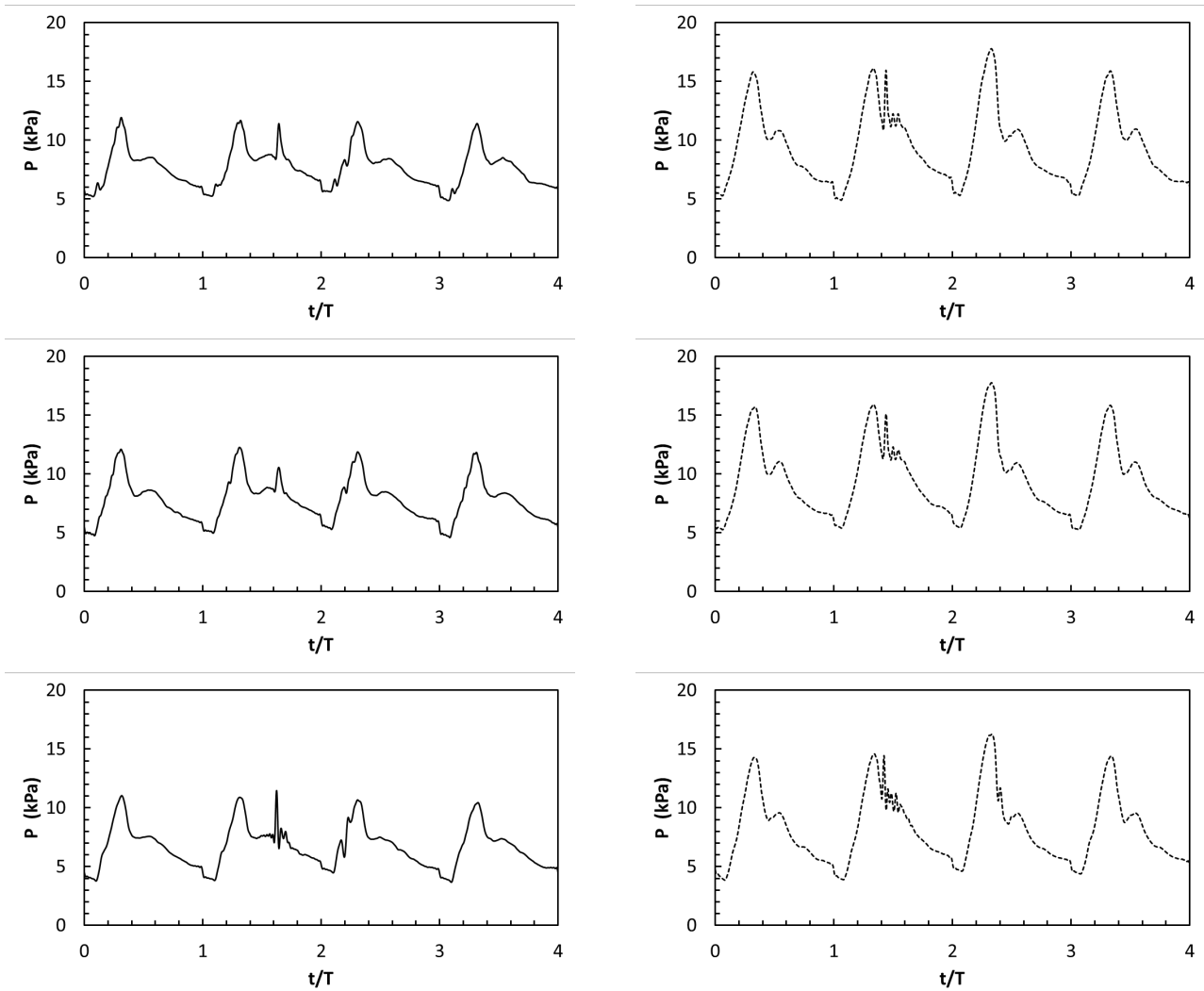


Fig. 4. Pressure waveform during the occlusion for the three sensors above the occlusion site (from top to bottom sensor 1, 2 and 3). Test 1 (left) and test 2 (right). The occlusion occurred during the 2nd cycle.

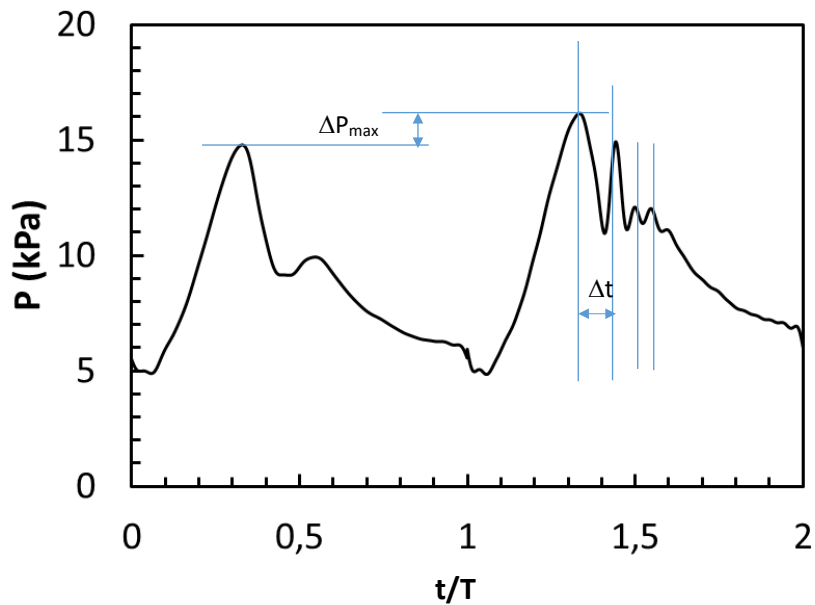


Fig. 5. Comparison of normal pressure waveform without occlusion (left) and during the occlusion (right) from sensor 1.

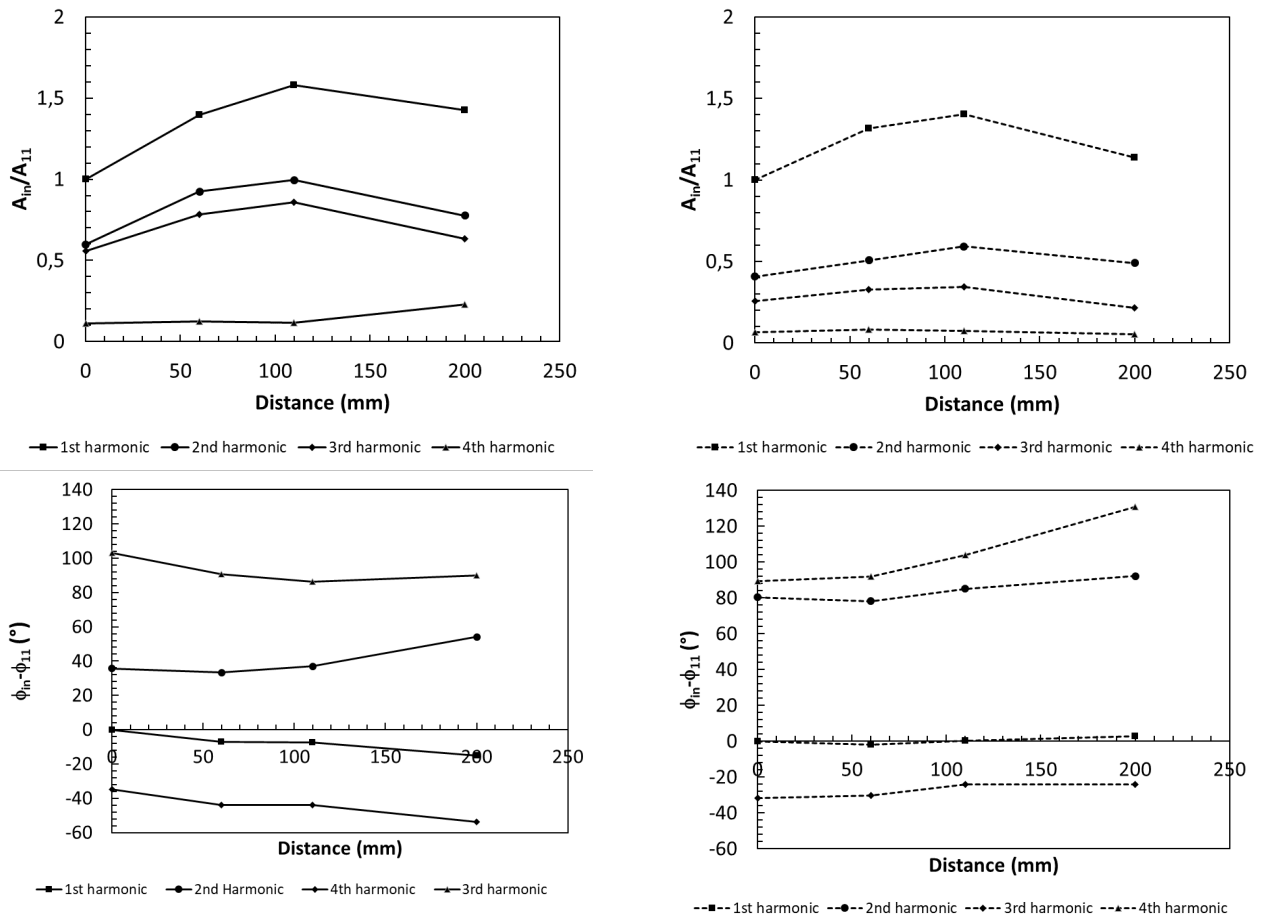


Fig. 6. Pressure amplitude (top), phase angles (bottom) along the aorta for the four first harmonics during the occlusion at the distal part of the thoracic aorta. Test 1 (left) and test 2 (right).

TABLE II
INSTANT OF THE MAXIMUM OF PRESSURE WITH OCCLUSION ALONG THE AORTA

Sensors	Sensor location d (mm)		Time of the maximum pressure t (ms)	
	Test 1	Test 2	Test 1	Test 2
1	0	0	312.5	315.0
2	60	55	309.5	313.0
3	110	110	303.5	309.0

IV. DISCUSSION

One of the supposed BTAR mechanisms is the result of an overpressure occurring at the aortic arch. This hypothesis suggests that blunt trauma leads to an aortic occlusion, resulting in a retrograde intraluminal pressure wave with a maximum effect at the aortic arch. There is extensive literature about the pressure propagation and reflection in the arterial tree of the human body in cardiovascular and haemodynamic research [20][29-35]. All these references described the shape of the pressure curve during a cardiac cycle. A first phase where the blood expelled from the heart into the aorta increase the pressure up to the systolic pressure (~15--17 kPa). Then the pressure decrease up to the closure of the aortic valve. After this closure, the pressure decrease more slowly due to the elasticity of the arterial wall that function like a blood tank to maintain a certain level of pressure and the distortion by the reflective wave created for instance by the aortic bifurcation. Among them, there are fewer results about the characterisation of the pressure wave along the aorta [33-35] or dealing with occlusion [33][36-38]. In impact biomechanics, some attempts were made to analyse the effect of an overpressure with a deceleration of the thorax but without replicating the real blood flow and without directly creating an occlusion of the flow [8][39].

The aim of the research program where the present study takes place was to develop a test bench that could reproduce the human blood flow with realistic conditions to study in details the mechanisms of overpressure due to a retrograde pressure wave in the aorta. The aim of the present work was to measure and describe the pressure wave along the aorta with and without an abdominal occlusion. In other words, to compare these two pressure waves and describe how a non-permanent but sudden occlusion modify the “normal” pressure wave.

For that purpose, a physiologic blood flow was reproduced with a pulsation of 1s (corresponding of a heart rate of 60 bpm) with a systolic pressure (maximum of pressure) between 11 and 16 kPa depending on the tested cardiopulmonary systems. This study has recorded simultaneous pressure measurements at different sites along the aorta and has compared several characteristics of the pressure wave propagation (amplitude, phase lags in the frequency domain). This first study shows that reproduction of the cardiovascular circulation is feasible and allowed measurement of flow and anterograde pressure wave. In addition, a sudden non-permanent aortic occlusion was created (at 0.6ms and 0.4ms for test 1 and 2 respectively) and has created a retrograde pressure wave in the thoracic aorta.

Pressure Pulse Analysis without occlusion

When blood is expelled from the heart, a pressure wave is generated and travels through the arterial tree. This original wave from the heart, i.e. the normal vascular response, is reflected on obstacles such as arterial bifurcations or occlusion and can even go backward. Thus, arterial pressure corresponds to the superposition of these original and reflected waves [40]. The shape and intensity of these pressure waves strongly depend on material geometry and properties such as wall stiffness, thickness, diameter or curvature of the vessels. Other factors such as pathologies or age can also affect the pressure wave. The pressure pulse is periodic and was analysed with a Fourier analysis, the first four harmonics of which are discussed.

The results showed that the mean pressure did not vary with the location because only a small fraction of the energy of the flow is dissipated by friction in the aorta due to the flow conditions. In contrast, the maximum value of all harmonics increased distally. These observations are in accordance with the cardiovascular literature and validate the experimental set-up. The data shows the changes in amplitude and phase angles for the different harmonics between the isthmus and the extremity of the aorta. This behaviour was already reported or described in cardiovascular literature (for instance [29][33-35]).

Variations (or absence of variations) in pressure amplitude and phase lags with distance and/or with frequency indicate the presence (or absence) of reflected waves in the arterial pulse. Differences were observed between the tested aortas and could be explained, partially, by the differences in tapered shape, and shape factor (see Table I). The aortic taper was reported as an important factor for the wave reflection [32]. The curvature of the arch was also more pronounced for the aorta used in test 1. The local variation of the section has a strong influence both on the fluids dynamics and on wave propagation. Due to the elastic behaviour of the arterial wall, the variation of the cross sectional area, A , has to be introduced in the fluid equation of continuity. Similarly, the velocity, c , of the wave depends on the geometrical data (the wall thickness and the diameter). The reflection of the pressure wave is due to the differences in the characteristic impedance at the site of reflection. The intensity of the reflection is also a function of c and A , the cross sectional area [33]. Consequently, a complete description of the pressure wave propagation requires the measurement of the cross sectional variation during the cardiac cycle.

Effect of the Occlusion of the Descending Aorta on the Pressure Pulse

The occlusion of the aorta at the distal extremity (above the iliac bifurcation that was not present on the present pig samples) clearly introduced strong distortion of the previous normal vascular pressure wave. A secondary pressure wave at higher frequency was observable on the signal. This wave created by the occlusion was found to move backwards since the moment of maximum pressure occurs later as one gets closer to the isthmus. The Fourier series decomposition was applied on this pressure wave and compared with the pressure without occlusion. It was shown that the occlusion produced an amplification in all harmonics with the distance along the aorta. Similar trends were reported by [33] during bilateral femoral artery occlusion by manual compression on patient. They reported that the femoral artery occlusion changed the character of the secondary systolic wave, which was increased in amplitude and more sharply peaked than without. Fig. 5 also shows an increase in amplitude and a strong distortion due to the pressure wave created by the occlusion. One main difference between these studies and the present work is that our occlusion was applied faster.

The maximum of pressure was also higher compared to the pressure without the occlusion. Nevertheless, this amplification of the pressure was relatively low (maximum pressure <20kPa) and did not produce a rupture of the arterial wall. Previous researches showed that a maximum pressure of 100kPa were associated to 50% of risk of aortic injury ([5][6]). This injury level was found with post-mortem human subject submitted to deceleration with an initial pressurisation of the arterial system at 10-13 kPa but without real fluid circulation, (the descending aorta was permanently closed). The over pressure observed in these studies was mainly due to the deceleration and of the associated fluid mass motion. In our tests, we only reproduce a sudden and non-permanent occlusion of the flow that create a retrograde pulse wave without fluid mass transfer. In hydraulics, the fact that the overpressure of a water hammer is lower with a compliant or flexible tube than a rigid one is well known. The aorta is a hyper-elastic material that may highly dampen pressure pulses.

In addition, the flow was rapidly resumed and this pressure wave rapidly vanished after two cardiac cycles, i.e. about 2 seconds (Fig. 4). A similar increase of pressure and rapid return to normal value after removing the occlusion was also described by [37]. However, it is difficult to conclude about the effect of an overpressure as a BTAR mechanisms. Several reasons can explain the fact that no rupture was observed before concluding on the effect or absence of effect of an overpressure. The duration of the occlusion are one of the factors that need to be further investigated. In particular, the compliance of the aorta is probably able to absorb this pressure wave. A longer occlusion could counterbalance the effect of the compliance due to the additional blood mass that will continue to arrive in the aorta due to the heart beat. Another factor that can influence the retrograde pressure wave is the location of the occlusion. The aortic occlusion experiments of [36] demonstrated that in order for reflections to reach the ascending aorta, they must be generated relatively close to the heart. This could explain the decrease in pressure amplitude increase at the proximal distance from the arch.

Limitations of the Study

In addition to the theoretical limitations discussed previously, this study has some limitations including the use of an animal model to reproduce the human circulatory system [33]. Firstly, there are some differences in the anatomy of the cardiopulmonary systems between pig and human. Although pig hearts are relatively similar to human hearts, there are subtle differences in the anatomy. The diameter of the great vessels are proportionally smaller in pigs than in humans. The comparison with human data showed that the diameter of the human ascending aorta is greater by 15-25%, and the descending aorta by 40%. In addition, the length of the descending aorta is shorter in pigs than in humans. The magnitude and velocity of the pressure depend on the length, wall thickness and the variation of the diameter along the aorta. Secondly, the aortic stiffness is an important factor for the pressure wave propagation, [41] found that the stiffness of young porcine aortic tissue shows good correspondence with human tissue aged <60 years. They performed a comparison for the ascending aorta of the circumferential and longitudinal stiffness based on a four fibre constitutive model for aortic mechanical behaviour. It also appears that both the human and porcine aortas are constructed so that failure occurs in the transverse direction [6]. Moreover, the animal cardiopulmonary system from young pigs are without atheromatous disease contrary to human. But blunt trauma of the aorta often reaches a young population without severe aortic atheromatous involvement as the model chosen [42].

In addition to the limitations about the use of animal instead of human tissues, there some points about the representativity of the model used in this work. One limitation of the test set-up is that the abdominal aortic bifurcation was absent. The retrograde pressure wave found in physiology originates essentially from this aortic bifurcation and it should be reproduce in future work. In physiology, 30% of the flow from the heart go through the supra-aortic trunk and its occur close to the supposed BTAR location. Consequently, this separation of the cardiac flow could be also important. We decided to keep as far as possible the surrounding viscera: lungs and pulmonary arteries (that were filled of fluid at the mean arterial pressure) to close as possible of the physiology and anatomy. Most of the research in literature had performed tests on isolated portion of the aorta, that to our opinion strongly limit the representativeness of the results.

The test set-up developed to reproduce a real blood flow also has limitations. The use of invasive instrumentation (pressure sensors) and the connection of the heart and the outlet of the aorta to the hydraulic system imply the possibility of having leaks that can appear during the tests and are difficult to control. There were other main limitations in the test bench compare to real blood flow.

First, is the use of a Newtonian fluid (i.e. water) to simulate the blood. Or the blood has a non-Newtonian behaviour. However, for vessels with a diameter larger than 0.1-0.5 mm, the blood can be considered as Newtonian. The dynamic viscosity of the blood becomes constant at high shear rates ($\dot{\gamma} > 100 \text{ s}^{-1}$) that

correspond to the shear rate in the aorta. Consequently the assumption of a constant dynamic viscosity, i.e., Newtonian fluid, is justified for the aorta (but it will not be the case for instance in smaller vessels). In this case, the density and the viscosity of the blood are $\rho \sim 1060 \text{ kg/m}^3$ and $\mu \sim 4 \cdot 10^{-3} \text{ Pa}\cdot\text{s}$ which is much higher than water and could influence the intensity of the pressure wave.

This leads to the second limitation of the bench, the similitude between the real blood flow and our simulated flow. The Reynolds $Re = uD/\nu$ and Womersley $Wo = D\sqrt{\omega}/\nu$ numbers are used to characterise a periodic flow. Both depend on the diameter D of the tube and the kinematic viscosity ν of the fluid. An exact similitude between water and blood flow should respect the equality of these numbers for the two fluids. This is not the case in the present study. However, the order of magnitude of the Reynolds and Womersley numbers are comparable and correspond to the same pattern of flow. For instance we have a Wo of 20 for the pig with water and > 13 for the human with blood that correspond to a same category of pulsatile flow [43]. Consequently, the results presented here are a good approximation of the fluid dynamics in the aorta. Nevertheless, we plan to use a blood-mimicking fluid (BMF) with a density and a kinematic viscosity similar to human blood at arterial shear rates in future experiments. The BMF will consist in a mixture of water-glycerol with a volume ratio of 60:40. At room temperature, this mixture has a density of $\rho \sim 1100 \text{ kg/m}^3$ and a viscosity of approximately $4.8 \cdot 10^{-3} \text{ Pa}\cdot\text{s}$.

Another limitation concerns the full characterisation of the pressure and blood wave. Theoretically, any pressure wave can be decomposed in a forward and backward (reflective) part. To separate and analyse precisely the components of the pressure wave, simultaneous measurement of velocity and pressure at the same location is required. This is not yet possible on the present bench. Moreover, an estimation of the wave velocity and of the impedance of the arterial wall is also needed. The main difficulty is that the arterial wall will strongly deform during the tests especially with the high-pressure wave expected during the occlusion. The measurement of the strain field on the external surface of the aorta or at least the variation of the diameter of the aorta at the pressure measurement location will be developed in future studies. This will allow access to the stress field (or the load of the arterial wall).

V. CONCLUSION

In order to study the mechanisms of BTAR due to an overpressure, an experimental study was performed to determine the effect of a sudden occlusion at the distal location of the descending thoracic aorta. Two pig aorta specimens were subjected to a pulsatile flow to represent the cardiac flow at a rate of 60 b.p.m. Pressure vs. time curves were derived from several measurement locations along the aorta from the isthmus to the outlet of the thoracic descending aorta.

The effect of the location along the descending aorta under physiological flow conditions, i.e., without perturbation, and when the extremity of the aorta was suddenly occluded were analysed. The physiological pressure wave was first analysed and described as a function of the location along the aorta. For that purpose, a Fourier series analysis was performed and the characteristics (amplitude and phase) of the 4th first harmonics of the pressure wave were discussed. The results showed variation, e.g. increase of the amplitude of each harmonics distally while the mean pressure remain constant, along the aorta that are comparable with the data reported in the literature. This validated our test set-up and served as a baseline for the comparison of the pressure wave after the temporary occlusion of the distal aorta.

The data showed that a pressure wave due to the sudden occlusion travelled backward to the isthmus at a velocity about 20-30 m/s. This pressure wave superimposed with the physiological pressure wave and amplified the maximum of the pressure. The increase of the maximum of pressure with distance along the aorta was found higher, by 10-14% in one case and less than 4% in the other case, with the occlusion than without. However, this pressure wave, that could be assimilated as a blood hammer effect vanished after two cardiac pulse since it was not a permanent occlusion. Moreover, the overpressure (around 18 kPa for the maximum recorded) was lower than those reported in the literature (around 100 kPa) to initiate a rupture of the aorta.

VI. ACKNOWLEDGEMENT

This research is partially funded by the “Action Incitative de Recherche AIR-2022” (Research incentive action) from the Research Vice-Presidency of the University Gustave Eiffel, France.

VII. REFERENCES

- [1] Richens D, Field M, Neale M, Oakley C. The mechanism of injury in blunt traumatic rupture of the aorta. *European Journal of Cardio-Thoracic Surgery*, 2002, 21(2):288-293.
- [2] Lundervall J. The mechanism of traumatic rupture of the aorta. *Acta Pathologica et Microbiologica Scandinavica*, 1964, 62:34-46.
- [3] Bertrand S, Cuny S, et al. Traumatic rupture of thoracic aorta in real-world motor vehicles crashes. *Traffic Injury Prevention*, 2008, 9:153-161.
- [4] Gomes VC, Silvestre GC, Queiroz A, Marques MA, Leão PP, da Silva ES. Biomechanical Analysis of Cadaveric Thoracic Aorta Zones: The Isthmus is the Weakest Region. *Annals of vascular surgery*, 2021, 77:263-273.
- [5] Forman J, Stacey S, Evans J, Kent R. Posterior acceleration as a mechanism of blunt traumatic injury of the aorta. *Journal of Biomechanics*, 2008, 41: 1359–1364.
- [6] Bass CR, Darvish K, et al. Material properties for modeling traumatic aortic rupture. *Stapp Car Crash Journal*, 2001, 45:143-160.
- [7] Hardy WN, Shah CS, Kopacz JM, Yang KH. Study of potential mechanisms of traumatic rupture of the aorta using insitu experiments. *Stapp car crash journal*, 2006, 50:247-266.
- [8] Hardy WN, Shah CS, Mason MJ, Kopacz JM, Yang KH, King AI. Mechanisms of Traumatic Rupture of the Aorta and Associated Peri-isthmus Motion and Deformation. *Stapp Car Crash Journal*, 2008, 52:233-265.
- [9] Greendyke RM. Traumatic rupture of aorta: special reference to automobile accidents. *Journal of American Medical Association*, 1966, 195(7):527-530.
- [10] Sevitt S. The mechanisms of traumatic rupture of the thoracic aorta. *British Journal of Surgery*, 1977, 64(3):166-173.
- [11] Viano DC. Biomechanics of non-penetrating aortic trauma: a review Proceedings of the 27th Stapp Car Crash Conference, SAE 831608, pp 109–114, 1983, San Diego, CA.
- [12] Parmley LF, Mattingly TW, Manion WC, Jahnke EJ. Non penetrating traumatic injury of the aorta. *Circulation*, 1958, 17(6):1086-1101.
- [13] Shah CS, Yang KH, Hardy W, Wang HK, King AI. Development of a computer model to predict aortic rupture due to impact loading. *Stapp Car crash Journal*, 2001, 45:1-22.
- [14] Marra S, Kennedy F, Kinkaid J, Fillinger M. Elastic and rupture properties of porcine aortic tissue measured using inflation testing. *Cardiovascular Engineering*, 2006, 6:125–133.
- [15] Mohan D, Melvin JW. Failure properties of passive human aortic tissue. II—biaxial tension tests. *Journal of Biomechanics*, 1983, 16(1):31–44.
- [16] Taylor, E. R. (1962) Thrombocytopenia following abrupt deceleration, ARL-TDR-62-30, 6571st ARL, AMD, AFSC, Holloman AFB, New Mexico.
- [17] Kivity Y, Collins R. Nonlinear wave propagation in viscoelastic tubes: application to aortic rupture. *Journal of Biomechanics*, 1974, 7(1):67-76.
- [18] Ray G, Liu YK, Davids N. Wall stress in curved aorta in blunt-chest trauma. *Proceedings of the 28th Annual Conference on Engineering in Medicine and Biology, Alliance for Engineering in Medicine and Biology*, September 20–24, vol. 17, 1975. p. 412.
- [19] Saito M, Ikenaga Y. et al. One-dimensional model for propagation of a pressure wave in a model of the human arterial network: comparison of theoretical and experimental results. *Journal of Biomechanical Engineering*, 2011, 133(12):121005.
- [20] Mynard JP, Kondiboyina A, Kowalski R, Cheung MMH, Smolich JJ. Measurement, Analysis and Interpretation of Pressure/Flow Waves in Blood Vessels. *Frontiers in Physiology*, 2020, 11:1085.
- [21] Powers WJ. Cerebral hemodynamics in ischemic cerebrovascular disease. *Annals of Neurology*, 1991, 29(3):231-240.
- [22] Rich GF, Lubanski RE, McLoughlin TM. Differences between aortic and radial artery pressure associated with cardiopulmonary bypass. *Anesthesiology*, 1992, 77(1):63-66.
- [23] Wilkinson IB, MacCallum H, Flint L, Cockcroft JR, Newby DE, Webb DJ. The influence of heart rate on augmentation index and central arterial pressure in humans. *The Journal of Physiology*, 2000, 525 Pt 1:263-270.
- [24] Karamanoglu M, Gallagher DE, Avolio AP, O'Rourke MF. Functional origin of reflected pressure waves in a multibranched model of the human arterial system. *American Journal of Physiology-Heart and Circulatory Physiology*, 1994, 267(5 Pt 2):H1681-1688.

- [25] Dark P, Little R, Nirmalan M, Purdy J. Systemic arterial pressure wave reflections during acute hemorrhage. *Critical Care Medicine*, 2006, 34(5):1497-505.
- [26] Bonfanti M, Franzetti G, Homer-Vanniasinkam S, Diaz-Zuccarini V, Balabani SA. Combined In Vivo, In Vitro, In Silico Approach for Patient-Specific Haemodynamic Studies of Aortic Dissection. *Annals of Biomedical Engineering*, 2020, 48(12):2950–2964.
- [27] Franzetti G, Diaz-Zuccarini V, Balabani S. Design of an In Vitro Mock Circulatory Loop to Reproduce Patient-Specific Vascular Conditions: Toward Precision Medicine. *Journal of Engineering and Science in Medical Diagnostics and Therapy*, 2019, 2(4):041004.
- [28] Alastruey J, Xiao N, Fok H, Schaeffter T, Figueroa CA. On the impact of modelling assumptions in multi-scale, subject-specific models of aortic haemodynamics. *Journal of the Royal Society Interface*, 2016, 13(119):20160073.
- [29] Swillens A, Segers P. Assessment of arterial pressure wave reflection: Methodological considerations. *Artery research*, 2008, 2:122-131.
- [30] Avolio AP. Multi-branched model of the human arterial system. *Medical and Biological Engineering and Computing*, 1980, 18(6): 709–718.
- [31] Van de Vosse FN, Stergiopoulos N. Pulse Wave Propagation in the Arterial Tree. *Annual Review of Fluid Mechanics*, 2011, 43:467-499.
- [32] Segers P, Mynars, J, Taelman L, Vermeersch S, Swillens A. Wave reflection: Myth or reality? *Artery Research*, 2012, 6:7-11.
- [33] Latham RD, Westerhof N, Sipkema P, Rubal BJ, Reuderink P, Murgu JP. Regional wave travel and reflections along the human aorta: a study with six simultaneous micromanometric pressures. *Circulation*, 1985, 72(6):1257-1269.
- [34] Luchsinger PC, Snell RE, Patel DJ, Fry DL. Instantaneous Pressure Distribution Along the Human Aorta. *Circulation Research*, 1964, 15(6):503-510.
- [35] O'Rourke MF, Blazek JV, Morreels Jr CL, Krovetz J. Pressure Wave Transmission along the Human Aorta. *Circulation Research*, 1968, 23(4):567-579.
- [36] Vandebos GC, Westerhof N, Elzinga G, Sipkema P. Reflection in systemic arterial system - effects of aortic and carotid occlusion. *Cardiovascular Research*, 1976, 10(5):565-573.
- [37] Khir AW, Zambanini A, Parker KH. Local and regional wave speed in the aorta: effects of arterial occlusion. *Medical Engineering & Physics*, 2004, 26: 23–29.
- [38] Khir AW, Parker KH. Wave intensity in the ascending aorta: effects of arterial occlusion. *Journal of Biomechanics*, 2005, 38:647–655.
- [39] Viano DC. Chest Impact Experiments Aimed at Producing Aortic Rupture. *Clinical Anatomy*, 2011, 24:339–349.
- [40] Nichols W, O'Rourke M, Vlachopoulos C. McDonald's blood ow in arteries: theoretical, experimental and clinical principles. CRC press, 2011. ISBN: 9780340985014.
- [41] de Beaufort H, Ferrara A, et al. Comparative Analysis of Porcine and Human Thoracic Aortic Stiffness. *European Journal of Vascular and Endovascular Surgery*, 2018, 55:560e566.
- [42] Pearson R, Philips N, Hancock R, et al. Regional wall mechanics and blunt traumatic aortic rupture at the isthmus. *European Journal of Cardio-Thoracic Surgery*, 2008, 34(3):616-622.
- [43] Womersley JR. Oscillatory Flow in Arteries. II: The Reflection of the Pulse Wave at Junctions and Rigid Inserts in the Arterial System. *Physics in Medicine & Biology*, 1958, 2:313-323.